Neuron
Article

Endogenous Cortical Rhythms Determine Cerebral Specialization for Speech Perception and Production

Anne-Lise Giraud,[1,2,3,4,*] Andreas Kleinschmidt,[4,5] David Poeppel,[6] Torben E. Lund,[7] Richard S.J. Frackowiak,[1,2,3,8,9] and Helmut Laufs[4]
[1]Inserm, U742, Paris, F-75005, France
[2]Université Pierre et Marie Curie-Paris 6, Paris, F-75005, France
[3]Département d'études cognitives, Ecole Normale Supérieure, Paris, F-75005, France
[4]Department of Neurology, J. W. Goethe University, Frankfurt am Main, D-60590, Germany
[5]INSERM U562, NeuroSpin, CEA, Gif-sur-Yvette, F-91091, France
[6]Cognitive Neuroscience of Language Laboratory, University of Maryland, College Park, MD 20742, USA
[7]Danish Research Centre for Magnetic Resonance, Copenhagen University Hospital, Kettegaard Alle 30, 2650 Hvidovre, Denmark
[8]Wellcome Trust, Institute of Neurology, UCL, London, WC1 3BG, UK
[9]IRCCS Santa Lucia, Rome, I-00179 Italy
*Correspondence: anne-lise.giraud@ens.fr
DOI 10.1016/j.neuron.2007.09.038

SUMMARY

Across multiple timescales, acoustic regularities of speech match rhythmic properties of both the auditory and motor systems. Syllabic rate corresponds to natural jaw-associated oscillatory rhythms, and phonemic length could reflect endogenous oscillatory auditory cortical properties. Hemispheric lateralization for speech could result from an asymmetry of cortical tuning, with left and right auditory areas differentially sensitive to spectro-temporal features of speech. Using simultaneous electroencephalographic (EEG) and functional magnetic resonance imaging (fMRI) recordings from humans, we show that spontaneous EEG power variations within the gamma range (phonemic rate) correlate best with left auditory cortical synaptic activity, while fluctuations within the theta range correlate best with that in the right. Power fluctuations in both ranges correlate with activity in the mouth premotor region, indicating coupling between temporal properties of speech perception and production. These data show that endogenous cortical rhythms provide temporal and spatial constraints on the neuronal mechanisms underlying speech perception and production.

INTRODUCTION

The evolution of spoken communication must have been constrained by neural mechanisms that were available for both perception and production (Liberman and Whalen, 2000; Gentilucci and Corballis, 2006). As speaking and understanding must be compatible with the performance limits of both auditory and motor systems, several theories have linked functional properties of perceptual and motor systems to speech capability. On the motor side, Frame/Content (F/C) theory (MacNeilage and Davis, 2000, 2001) proposes that the features of elementary production units, i.e., syllables, are determined by mechanical properties of the speech apparatus, e.g., natural oscillatory rhythms. On the perceptual side, the Asymmetric Sampling in Time theory (AST; Poeppel, 2003) proposes that auditory cortices preferentially sample at rates tuned to fundamental speech units. While the left auditory cortex would integrate auditory signals preferentially into ~20–50 ms segments that correspond roughly to the phoneme length, the right auditory cortex would preferentially integrate over ~100–300 ms and thus optimize sensitivity to slower acoustic modulations, e.g., voice and musical instrument periodicity, speech prosody, and musical rhythms (Schneider et al., 2005; Belin et al., 2004; Peretz and Zatorre, 2005).

Common to both theories is that they link speech processing to neural oscillations. Such oscillations could emerge in the context of input processing or output generation, in which case the associated neural activities would reflect the structure of speech. However, neural oscillations are abundant in ongoing spontaneous brain activity patterns that are unrelated to any specific input or output context. It therefore appears conceivable that oscillations at speech-relevant frequencies could constitute intrinsic properties of specialized brain structures, thus accounting for the fact that speech sounds the way it does. In this case, a hypothesis emerges that the strength or power of oscillations in speech-relevant frequency bands is linked to regional activity in areas specialized for speech perception and production, even in the absence of explicit speech perception and production. We tested the

prediction of intrinsic coupling by studying the association between *spontaneous* modulations of power in appropriate frequency bands, as recorded by EEG, with local synaptic activity, as registered by simultaneous functional magnetic resonance imaging (fMRI). We extracted the temporal modulation of spectral EEG information in a priori specified bands of interest (Laufs et al., 2003, 2006). We convolved the power time courses in these bands with hemodynamic response properties and used the resulting regressors (see Figure S1 available online) to interrogate spontaneous fMRI signal fluctuations for correlated local brain activity changes over time. Crucially, this approach involved no experimental modulation of auditory input, no perceptual task, and no speech output, thus revealing purely intrinsic coupling between specific spontaneous brain oscillatory frequencies and local brain activity levels.

RESULTS

We determined the topographical distribution of spontaneous cortical activity modulations associated with each of the two temporal domains of interest for speech perception. The two integration windows correspond to (1) chunking into ~20–50 ms segments—the narrower integration window—approximating 20–50 Hz EEG activity, and (2) chunking into ~150–300 ms segments—the larger integration window—approximating 3–6 Hz EEG activity (Figure 1A). If different intrinsic cortical oscillation frequencies are associated with differential temporal analysis by right and left auditory cortices, long-term (measured over 40 min) fluctuations of EEG power in each band should correlate with auditory cortex activity changes, and the patterns should reflect hemispheric specialization even in the absence of speech input.

AST Hypotheses and Spontaneous EEG Rhythms

Across the brain the most significant correlation of fMRI signal with 3–6 Hz power fluctuations occurred in superior temporal cortices. In keeping with AST, this effect is located in Heschl's gyrus in the right hemisphere (spatial coordinates in MNI standard space: 37 −28 14, Z = 11.2, Figure 1B), overlapping primary auditory cortex. In contrast, on the left, the effect occurs more rostrally/ventrally and thus not in colocalization with Heschl's gyrus. In both lateral and medial Heschl's gyri, we observed a significant right hemispheric advantage across subjects.

In the next step, we tested the second central tenet of AST theory—that left auditory cortex, overlapping with Heschl's gyrus, is preferentially tuned to short acoustic segments. We analyzed fMRI signal fluctuations related to EEG power in the 28–40 Hz band. This band corresponds to 25–35 ms segments, and was chosen because of previous reports that left auditory cortex does not respond to acoustic segments shorter than 25 ms (Boemio et al., 2005). As predicted, we detected a significant correlation between EEG power fluctuation in this frequency band and synaptic activity, indexed by fMRI, in superior temporal cortices at the lateral/rostral edge of primary

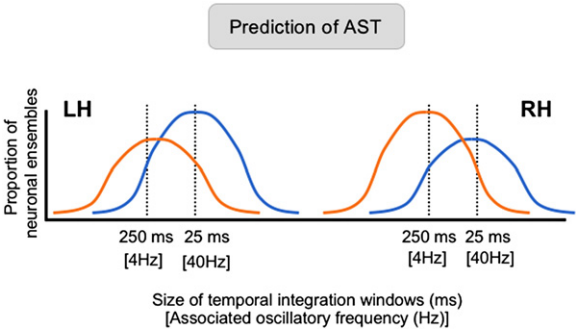

Figure 1. AST Theory

AST predicts that differential proportions of neurons sampling the auditory signal at two different rates in each auditory cortex account for functional auditory asymmetries.

auditory cortex (Figure 2A), with a left/right asymmetry trend that was not significant across subjects. In keeping with the prediction of AST, we observed a double dissociation profile in lateral Heschl's gyrus with right hemisphere dominance for the 3–6 Hz band and a left hemisphere advantage for 28–40 Hz. Direct comparisons between bands indicated that 3–6 Hz EEG power correlated significantly more with activity in right Heschl's gyrus than did the 28–40 Hz band (48 −20 14, Z = 3.76). Because EEG power was overall greater in the 3–6 Hz than the 28–40 Hz band, the opposite contrast (28–40 Hz versus 3–6 Hz) resulted in no significant effects. However, correlation nearly reached significance just posterior to Heschl's gyrus in the left planum temporale (−48 −28 10, Z = 2.11).

Analysis over five discontinuous frequency bands (3–6 Hz, 9–12 Hz, 15–18 Hz, 20–25 Hz, and 28–40 Hz) (Experiment 1) established the spectral specificity of the effects (Figure 2B). In lateral Heschl's gyrus, we found that positive correlations were restricted to our two bands of interest, with the exception of a right-lateralized effect at 9–12 Hz. This effect suggests that the slow window of integration may be a little larger than postulated, i.e., 100–300 ms instead of 150–300 ms as hypothesized. This difference is coherent with previous psychophysical and physiological observations, e.g., that speech becomes unintelligible when syllables become shorter than 100 ms. In other bands, and even for 9–12 Hz in left lateral Heschl's gyrus, neural activity correlated negatively with EEG fluctuations. Over the entire brain, we found a significant negative correlation between the 20–25 Hz band and neural activity in right auditory cortex, indicating greater activity whenever 20–25 Hz band power decreased (Laufs et al., 2003, 2006). This negative correlation at 20–25 Hz EEG may be due to desynchronization in frequencies below the 28–40 Hz band (Ross et al., 2005). These control results emphasize the spectral selectivity of the correlations found and their congruence with the frequency bands hypothesized by AST.

A second experiment (Experiment 2) performed in eight male subjects confirmed that correlation with 3–6 Hz spontaneous activity was more pronounced in right than

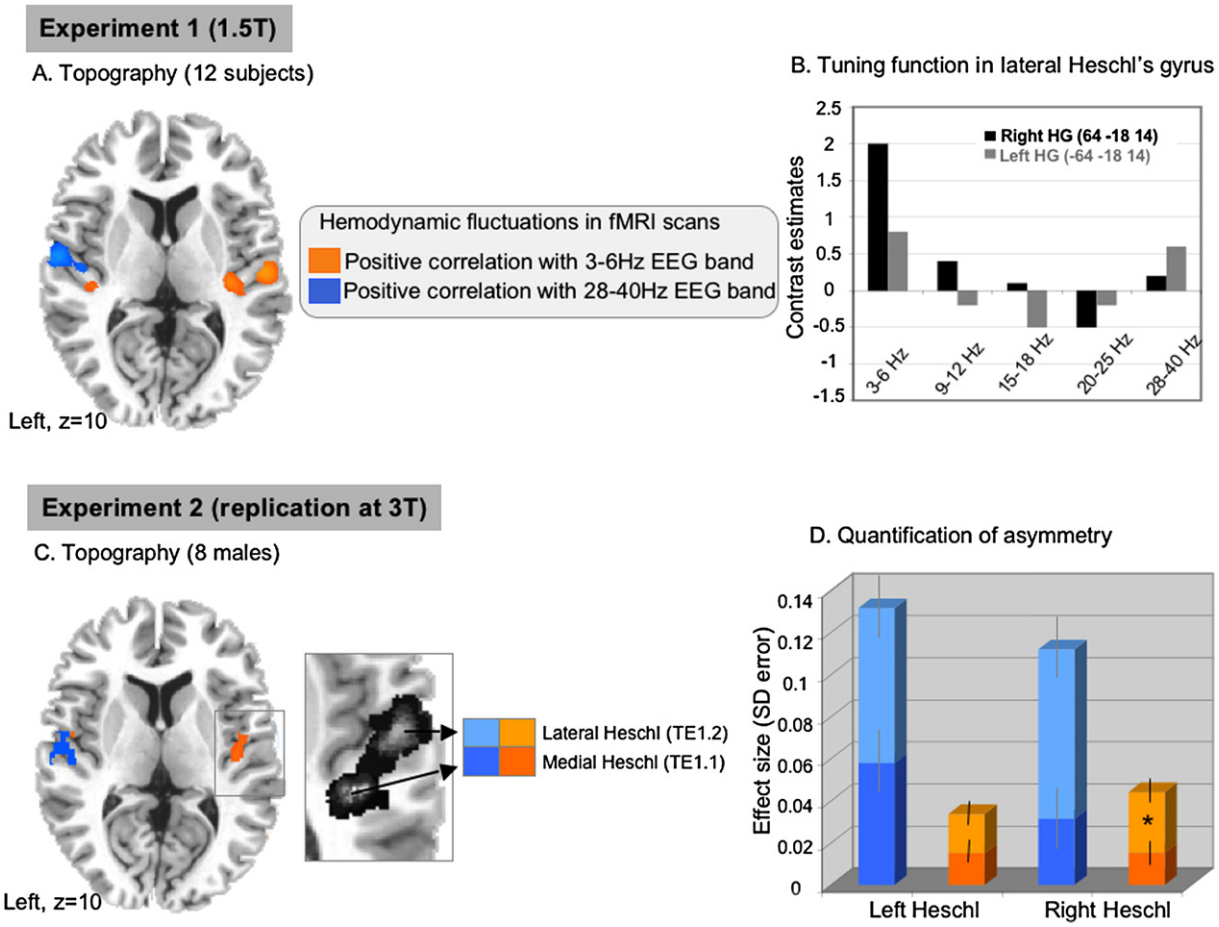

Figure 2. Correlations between EEG and Hemodynamic (fMRI) Fluctuations in Auditory Cortices

(A and B) Group results from Experiment 1 (fixed-effects statistics): 18 sessions from 12 subjects acquired on a 1.5 T MRI scanner. (A) Topography of 3–6 Hz-associated and 28–40 Hz-associated fMRI signal in auditory cortices is rendered on transversal slice, showing that fluctuations in these rhythms are associated with activity modulations that overlap with right and left Heschl's gyri, respectively. (B) Across five bands of EEG power, significant positive correlations with BOLD activity in auditory cortices were only observed for those hypothesized by AST.

(C and D) Group results from Experiment 2 (random-effects statistics): eight 33 min sessions from eight male subjects acquired on a 3T MRI scanner. (C) Rendering on a transverse slice shows the same global pattern as in Experiment 1 in auditory cortices. (D) A double dissociation profile was confirmed when measuring the effects in each individual within anatomically defined volumes of interest (TE 1.1 and TE 1.2, after Eickhoff et al., 2005, shown in the quadrant for the right auditory cortex). A lateralization effect was associated with a $p = 0.051$ for the 3–6 Hz rhythm in TE 1.2. There was no statistically significant lateralization effect of 28–40 Hz rhythm, although a trend is clearly visible. The index of asymmetry was strongest for 3–6 Hz at the lateral border of Heschl (TE 1.2), and strongest for 28–40 Hz at the medial border of Heschl (TE 1.1).

left Heschl's gyrus, with the opposite profile for 28–40 Hz band activity. The topography was similar in both experiments (Figure 2C). Because we used a more conservative random-effects analysis for replication in this second experiment, activity in Heschl's gyrus was associated with lower Z scores than in the first (left Heschl $Z = 2.99$ [$p < 0.05$], right Heschl $Z = 2.17$ [$p < 0.05$] for 28–40 Hz; left Heschl $Z = 1.90$, right Heschl $Z = 3.06$ [$p < 0.001$] for 3–6 Hz). These statistical levels are acceptable for a hypothesis-driven volume of interest replication analysis. We extracted individual values within two cytoarchitectonic maps of auditory cortex, TE 1.1 and TE 1.2, which correspond to the medial and lateral parts of Heschl's gyrus, respectively. We confirmed global asymmetric profiles. Asymmetry was present in medial Heschl for 28–40 Hz (as a trend) and in lateral Heschl for 3–6 Hz ($p = 0.051$, Figure 2D). These quantitative results indicate that both rhythms are correlated with activity on both sides, with a trend for better correlation with the slower rhythm in right Heschl's gyrus and correlation with the faster rhythm in left.

F/C Hypotheses and Spontaneous EEG Rhythms

Finally, we address the hypothesis derived from the F/C theory of speech production (MacNeilage and Davis, 2000, 2001) that syllabic rhythms, i.e., those around 4 Hz, are related to intrinsic motor properties of the vocal apparatus. We found that power in the 3–6 Hz band was significantly correlated with synaptic activity in the inferior

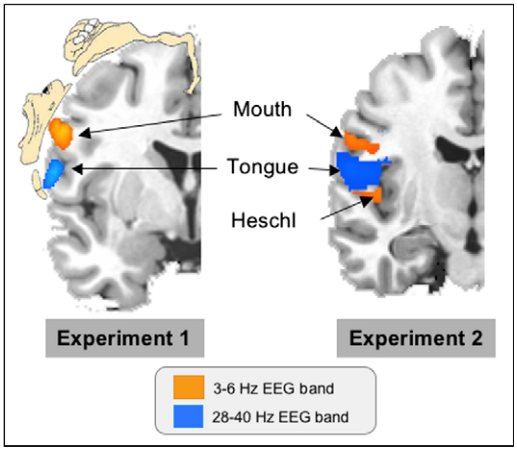

Figure 3. Correlations between EEG and Hemodynamic (fMRI) Fluctuations in Premotor Cortices

Superimposition of EEG/fMRI correlations in 3–6 Hz (yellow) and 28–40 Hz (blue) bands with the motor "homunculus" on a transverse slice illustrates that right motor activations are situated close to the mouth and tongue motor regions, two regions that are necessary for speech production. The motor homunculus illustrates large-scale somatotopy of primary motor cortex in a location just posterior to the transverse section selected. Left panel corresponds to Experiment 1 and right panel to Experiment 2. Clusters are rendered on the left side, although no consistent lateralization effect was observed.

motor region, overlapping an area involved in generating mouth movements (Figure 3, left panel). We also found correlations between neural activity and EEG fluctuations in the 28–40 Hz band in an adjacent region located more ventrally, overlapping a region implicated in preparation of tongue movements. We detected no asymmetries in motor cortical activity in any EEG rhythm domain (Figure 4). The relative location of 3–6 Hz versus 28–40 Hz along the motor strip, with a slightly more dorsal location for syllabic (−56 −8 40, Z = 3.16) as compared with phonemic (−50 −6 36, Z = 4.02) rhythms, was replicated in Experiment 2 (Figure 3, right panel).

Nonhypothesized Observations

In addition to the correlation of 3–6 Hz oscillations with right Heschl's gyrus activity, we found a relationship to neural activity in a more anterior and ventral region of the left temporal lobe. The effect was greater in the 3–6 Hz band than at higher frequency, and was more pronounced in the right cortex than the left cortex (Figure 4, plot A). This contrasts with the profile in auditory cortex near Heschl's gyrus, which showed a right dominance for that same 3–6 Hz band.

Finally, both 3–6 Hz and 28–40 Hz rhythms correlated with neural activity in regions outside those directly related to speech comprehension and production. Both rhythms correlated with visual cortex activity and more dorsal/frontal parts of the premotor region. In the second experiment, 3–6 Hz rhythm was associated with significant activity of the left hippocampal gyrus (−40 −40 −12, Z = 3.35), which is consistent with many previous studies describing the hippocampus as a source of theta oscillations (Vertes, 2005).

DISCUSSION

In this study we tested whether functional brain asymmetries in speech processing could be accounted for by differential intrinsic sampling properties in each auditory cortex, as predicted by AST and earlier related models (Zatorre and Belin, 2001). AST suggests that both primary auditory cortices sample with fine grain, but surrounding auditory areas chunk the initial input with different temporal windows, a narrow one in the left hemisphere and a broader one in the right. On the left, integration of auditory signals into ~20–50 ms segments optimally resolves the fine acoustic structure critical for phonetic contrast perception in speech (Rosen, 1992). Such differential functionality could underpin left hemispheric phonemic-level speech processing (Scott and Johnsrude, 2003; Friederici and Alter, 2004). Integration into ~100–300 ms segments in right auditory cortex optimizes extraction of slow information, thus promoting processing of periodicity, voice, prosody, and music (Schneider et al., 2005; Belin et al., 2004; Peretz and Zatorre, 2005). In agreement with the AST, slow fluctuations in 3–6 Hz EEG rhythms correlated most strongly with spontaneous neural activity in the right auditory region, while higher-frequency fluctuations in the 28–40 Hz range showed left hemispheric predominance. In both experiments, EEG power was not equal in the two bands of interest; power was higher for theta than gamma in the first and higher for gamma than theta in the second experiment. Despite such differential sensitivity, which prevents direct comparisons across bands, we replicated a double dissociation profile with higher 3–6 Hz-associated brain activity in right than left auditory cortex and higher 28–40 Hz-associated activity in left than right auditory cortex.

Our results agree with previous fMRI data showing that the right superior temporal region responds more than the left to 100–300 ms acoustic segments (Boemio et al., 2005). This latter finding in itself can be accounted for by stimulus- or task-related auditory functional asymmetries. Such an account would not hold for our findings here because our results relate functional asymmetries to local intrinsic neuronal properties. We explicitly avoided stimulus- and task-driven confounds by assessing spontaneous activity fluctuations during 40 min. of continuous acoustic input uncorrelated with the target phonemic and syllable-related frequencies (see Experimental Procedures). This refinement is critical as in this setting our results indicate asymmetric implementation of auditory sampling via distinct *intrinsic* oscillation rates in separate neuronal populations. The inference is that there are hard primary physiological constraints at the level of temporal integration of auditory signals. Thus, we reinterpret previous results (including those of Boemio et al., 2005) by relating stimulus-associated tuning to the temporal structure of spontaneous activity in speech-processing brain regions.

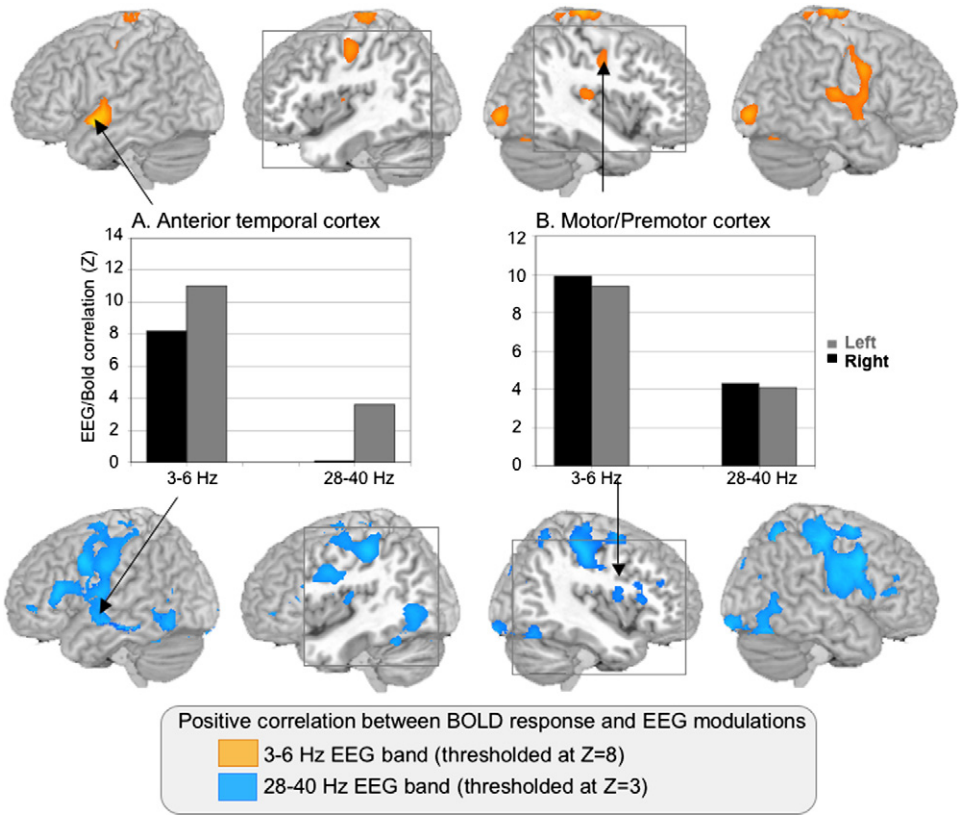

Figure 4. Correlations between EEG and Hemodynamic (fMRI) Fluctuations over the Whole Brain

Hemodynamic correlates of 3–6 Hz (yellow, thresholded at Z = 7) and 28–40 Hz (blue, thresholded at Z = 3.5) band modulation of surface EEG during fMRI scanning. Different thresholds were used for each band as the energy in the 28–40 Hz band was lower than that in the 3–6 Hz band. This yielded a higher interindividual variability for the 28–40 Hz compared with the 3–6 Hz band (hence, lower overall statistical thresholds in group correlations). Activations overlapping with Heschl's gyrus are shown on right and left sections (gray frames). Mean levels of EEG/fMRI correlations are indicated in middle row panels in three key regions for speech perception and production: (A) the anterior temporal cortex; (B) the mouth premotor region.

Our findings are in accord with micro-anatomical descriptions of lateralized features of the auditory cortices. Left auditory and language-associated regions contain a greater number of large pyramidal cells (Hutsler and Galuske, 2003) that typically display fast rhythmic bursting at gamma rates (Gray and McCormick, 1996; Traub et al., 2003). Conversely, there are a greater proportion of smaller pyramidal cells in the right auditory cortex. Both macro-anatomical (Dorsaint-Pierre et al., 2006) and micro-anatomical features bias left hemispheric structures to chunk the flow of auditory signals at a higher frequency, and bias right sided structures to integrate it into longer periods.

Our results speak to a neural implementation of two *discontinuous* auditory integration windows, each tuned to critical temporal units of speech. Across five discontinuous frequency bands, used as multiple regressors to interrogate the fMRI time series, only power in the two bands of interest showed a positive correlation with neural activity in auditory cortices. An essential aspect of a sensory analysis scheme involving multiple timescales is discontinuity in structural properties. Our results therefore indicate that multiple timescale auditory analysis is implemented by a spatial right-left dissociation and a structural high-frequency/low-frequency dissociation operating in a single cortical site, as predicted by AST theory (Figure 2D).

The frequency bands posited by AST overlap common EEG band boundary definitions, i.e., theta (4–7 Hz) and gamma (30–50 Hz), but are not identical to them, despite previous suggestions to the contrary (Boemio et al., 2005). Our results do not relate to classical auditory evoked events (Engel et al., 2001), as they are grounded in an analysis of spontaneous EEG fluctuations measured continuously on a long timescale (two 20 min sessions) that describe long-range activity relationships between distant neuronal populations (Mukamel et al., 2005). This intrinsic functional design remains compatible with an additional influence from stimulus-driven adaptive mechanisms, e.g., gliding integration mechanisms, that tune or reset integration windows via sensory input within the two frequency domains we identify (White and Plack, 1998; Bair and Movshon, 2004; Ross et al., 2005; Lakatos et al., 2007; Luo and Poeppel, 2007).

Activity in the left anterior temporal cortex also correlated positively with 3–6 Hz EEG fluctuations. However,

unlike the 3–6 Hz activity in auditory cortex near Heschl's gyrus, this more anterior effect had a left dominance (Figure 4, plot A). The location and physiological profile of this effect was not predicated by AST theory but may be relevant to it. While 3–6 Hz is the preferred primary sampling frequency of right auditory cortex, the same band might also function as a higher-order temporal integrator of shorter auditory segments in left temporal cortex. In support of this idea is the fact that speech remains intelligible if segmented into reversed chunks of up to 100 ms in duration (Saberi and Perrott, 1999), suggesting that a large temporal window plays a supra-segmental integrative role in speech comprehension. Our hypothesis that 3–6 Hz activity reflects a second-order left temporal cortical mechanism (Freeman and Holmes, 2005; Canolty et al., 2006) is supported by the finding of a (primary) left-sided sampling mechanism at higher frequency overlapping with Heschl's gyrus, i.e., in a region closer to primary auditory cortex. Thus, in addition to a right-left dissociation for the two frequency windows, we find a posterior/anterior spatial distribution of the two frequency bands in left temporal cortex, with a primary fast sampling mechanism in or near left primary auditory cortex and a slower integrative mechanism in a more anterior region. This latter mechanism may function to concatenate the segmented output from left auditory cortex, transforming it into symbolic speech units. In accord with this formulation, the anterior temporal region contains topographically organized maps of vowels and syllables (Rauschecker and Tian, 2000; Obleser et al., 2006).

From an evolutionary and teleological perspective, neural mechanisms for speech input processing and output generation should share common neural carrier frequencies (Hickok and Poeppel, 2004; Lagarde and Kelso, 2006). In support of this notion, we observe that both 3–6 Hz and 28–40 Hz frequency domains correlate with neural activity in both auditory and premotor cortices. The 3–6 Hz band power in the lower part of the motor cortex offers a direct neural underpinning for the F/C theory of speech that assumes syllables are phylogenetically and ontogenetically determined by natural mandibular cycles occurring at about 4 Hz. We show that spontaneous neural oscillations at this frequency, i.e., the dominant syllabic rate, are associated with cortical activity in regions underpinning both speech perception and production. Furthermore, we find in two independent data sets that the 28–40 Hz band correlates with a peak of activation in a slightly more ventral location than the 3–6 Hz band, in a region that controls movements of the tongue (Figure 3). As tongue positioning is critical to articulation and discriminates between consonant families in speech production, it is conceivable that the auditory system has adapted its sensitivity to natural constraints imposed by the articulatory motor system. In keeping with symmetrical speech motor commands, we found no consistent right/left asymmetries in motor regions (Figure 4), although the distribution of 3–6 Hz band activity was more rostral in the left hemisphere and colocalized in part with Broca's area. Selective rhythmic activity in the premotor region is compatible with the view that articulatory movements may be the primary promotors of language (Liberman and Whalen, 2000).

Together, our findings support, refine, and extend theories linking speech regularities to spontaneous oscillatory properties of brain systems for speech perception and production. In relation to AST theory, we show that (1) spontaneous power fluctuations of 3–6 Hz and 28–40 Hz intrinsic oscillations are paralleled by specific modulations of neural activity in auditory/temporal cortices; and (2) auditory activity in regions overlapping Heschl's gyrus is more prominently associated with the 3–6 Hz band in the right hemisphere and the 28–40 Hz band in the left. With respect to F/C theory, we show that ventral premotor cortex activity is correlated with spontaneous neural oscillations at the syllabic rate of natural speech. These results suggest that basic neuronal constraints on auditory processing and motor output, including hemispheric specialization, parallel major acoustic temporal characteristics of speech. They emphasize the role of common cortical oscillatory frequency bands for speech production and perception and thus provide a brain-based account for the phylogenetic emergence and shaping of speech from available neural substrates.

EXPERIMENTAL PROCEDURES

Twenty healthy subjects underwent simultaneous EEG and blood oxygen level-dependent (BOLD) fMRI during eyes-closed rest. All subjects wore ear defenders to attenuate scanner noise, and were requested to stay awake and avoid movement.

Twelve of them (six male and six female subjects, age range 26–35, median 31.5 years) participated in a first experiment consisting of, in two successive 20 min sessions, EEG (BrainAmp MR, Brainproducts, Munich, Germany) recorded using a 32 channel EEG cap (Falk Minow Services, Herrsching-Breitbrunn, Germany) including an ECG electrode. In each session, 300 echoplanar fMRI image volumes were acquired on a 1.5 T Magnetom Vision (Siemens, Erlangen, Germany) consisting of 19 contiguous transverse slices covering almost the entire cerebrum (echo time 50 ms, voxel size 3.44 × 3.44 × 4 mm^3, 1 mm interslice gap). Time of acquisition for a single volume was 2.8 s followed by a 1.2 s gap before acquisition of the next, yielding a 4 s TR. Session data were discarded if wakefulness could not be maintained, which resulted in 18 sessions available for analysis.

A replication experiment was run on eight male subjects (age range 25–35, median 29.6 years) on a 3T Siemens Trio (1000 EPI volumes each, TR/TE = 2 s/30 ms, 64 × 64, FOV 192 mm, 33 slices of 3 × 3 × 3 mm^3 plus 1 mm interslice gap, no pause between volumes). EEG was recorded simultaneously as described above, with wires guided in the z axis to the digitizer inside the bore, which operated time-locked with the scanner clock and hence improved artifact reduction and resulted in higher EEG quality (Mandelkow et al., 2006).

Acoustic input was analyzed by spectro-temporal analysis of MRI scanner noise. The scanner produced a constant auditory input during data acquisition corresponding roughly to white noise (0 to 6 kHz) modulated at TR rate, with a second major modulation corresponding to the number of slices per volume (Figure S2 for scanner noise-detailed analysis in Experiment 2). None of the temporal modulations present in the scanner noise spectrally overlapped with our bands of interests (3–6 Hz, 28–40 Hz), ruling out possible interference between input (noise in delta and alpha bands), output (cortical oscillations in theta and gamma bands), and rhythmic activity driven by scanner noise.

Both data sets were analyzed using Statistical Parametric Mapping (SPM2, http://www.fil.ion.ucl.ac.uk/spm) for spatial preprocessing, including realignment, normalization, and smoothing (10 mm full-width at half-maximum isotropic Gaussian Kernel) to facilitate a group analysis. After imaging and pulse artifact subtraction (Vision Analyzer, Brainproducts), we used a short time Fourier Transform (frequency/temporal resolution of 1 Hz/s, moving average with 33% overlap, MATLAB, Mathworks, Inc., Sherborn, MA) to calculate power time courses for 3–6, 9–12, 15–18, 20–25, and 28–40 Hz for the frontocentral electrode (equidistant to the temporal lobes) referenced to the mean of the two occipital electrodes (i.e., most distant position). Although this setting is not optimal for measuring responses in auditory cortices, it was considered essential to avoid any lateralizing bias in the EEG signal used to analyze the fMRI data. The effects observed in auditory cortices with this choice of electrode were separately confirmed using independent signals from temporal electrodes.

Time courses of power in the aforementioned EEG bands were convolved with the hemodynamic response function (Figure S1), downsampled to the middle of each image volume acquisition, and then used as regressors in a general linear model (using SPM). Parameters obtained from realignment were modeled as confounds to account for subject motion effects. Statistical inferences were performed via group t tests for the bands of interest. Modeling the 9–12 and 15–18 Hz frequency bands of no interest (in this study) served to control for non-band-specific power changes (e.g., those caused by artifacts) and to explain variance in the data associated with other brain processes (Laufs et al., 2006). We report fixed-effects statistics for the first study (for exploratory purposes). The second data set was analyzed using second-level random-effects statistics based on the individuals' contrast images, and performed by means of a voxel-wise t test (Friston et al., 1999).

Supplemental Data

The Supplemental Data for this article can be found online at http://www.neuron.org/cgi/content/full/56/6/1127/DC1/.

ACKNOWLEDGMENTS

We thank Yves Burnod, Etienne Koechlin, Christian Kell, and Christian Lorenzi for technical help and useful comments on the manuscript. This research was funded by the Bundesministerium für Bildung and Forschung (Germany). R.S.J.F. was funded by a Wellcome Trust program grant (Ref: 075696Z/04/Z) and a Chaire d'excellence from Agence Nationale de la Recherche (France); A.L.G. was funded by CNRS (France).

Received: February 20, 2007
Revised: July 13, 2007
Accepted: September 11, 2007
Published: December 19, 2007

REFERENCES

Bair, W., and Movshon, J.A. (2004). Adaptive temporal integration of motion in direction-selective neurons in macaque visual cortex. J. Neurosci. *24*, 7305–7323.

Belin, P., Fecteau, S., and Bedard, C. (2004). Thinking the voice: neural correlates of voice perception. Trends Cogn. Sci. *8*, 129–135.

Boemio, A., Fromm, S., Braun, A., and Poeppel, D. (2005). Hierarchical and asymmetric temporal sensitivity in human auditory cortices. Nat. Neurosci. *8*, 389–395.

Canolty, R.T., Edwards, E., Dalal, S.S., Soltani, M., Nagarajan, S.S., Kirsch, H.E., Berger, M.S., Barbaro, N.M., and Knight, R.T. (2006). High gamma power is phase-locked to theta oscillations in human neocortex. Science *313*, 1626–1629.

Dorsaint-Pierre, R., Penhune, V.B., Watkins, K.E., Neelin, P., Lerch, J.P., Bouffard, M., and Zatorre, R.J. (2006). Asymmetries of the planum temporale and Heschl's gyrus: relationship to language lateralization. Brain *129*, 1164–1176.

Eickhoff, S.B., Stephan, K.E., Mohlberg, H., Grefkes, C., Fink, G.R., Amunts, K., and Zilles, K. (2005). A new SPM toolbox for combining probabilistic cytoarchitectonic maps and functional imaging data. Neuroimage. *25*, 1325–1335.

Engel, A.K., Fries, P., and Singer, W. (2001). Dynamic predictions: oscillations and synchrony in top-down processing. Nat. Rev. Neurosci. *2*, 704–716.

Freeman, W.J., and Holmes, M.D. (2005). Metastability, instability, and state transition in neocortex. Neural Netw. *18*, 497–504.

Friederici, A.D., and Alter, K. (2004). Lateralization of auditory language functions: a dynamic dual pathway model. Brain Lang. *89*, 267–276.

Friston, K.J., Holmes, A.P., and Worsley, K.J. (1999). How many subjects constitute a study? Neuroimage *10*, 1–5.

Gentilucci, M., and Corballis, M.C. (2006). From manual gesture to speech: A gradual transition. Neurosci. Biobehav. Rev., in press.

Gray, C.M., and McCormick, D.A. (1996). Chattering cells: superficial pyramidal neurons contributing to the generation of synchronous oscillations in the visual cortex. Science *274*, 109–113.

Hickok, G., and Poeppel, D. (2004). Dorsal and ventral streams: a framework for understanding aspects of the functional anatomy of language. Cognition *92*, 67–99.

Hutsler, J., and Galuske, R.A. (2003). Hemispheric asymmetries in cerebral cortical networks. Trends Neurosci. *26*, 429–435.

Lagarde, J., and Kelso, J.A. (2006). Binding of movement, sound and touch: multimodal coordination dynamics. Exp. Brain Res. *173*, 673–688.

Lakatos, P., Chen, C.M., O'Connell, M.N., Mills, A., and Schroeder, C.E. (2007). Neuronal oscillations and multisensory interaction in primary auditory cortex. Neuron *53*, 279–292.

Laufs, H., Krakow, K., Sterzer, P., Eger, E., Beyerle, A., Salek-Haddadi, A., and Kleinschmidt, A. (2003). Electroencephalographic signatures of attentional and cognitive default modes in spontaneous brain activity fluctuations at rest. Proc. Natl. Acad. Sci. USA *100*, 11053–11058.

Laufs, H., Kleinschmidt, A., Beyerle, A., Eger, E., Salek-Haddadi, A., Preibisch, C., and Krakow, K. (2006). EEG-correlated fMRI of human alpha activity. Neuroimage *31*, 1408–1418.

Liberman, A.M., and Whalen, D.H. (2000). On the relation of speech to language. Trends Cogn. Sci. *4*, 187–196.

Luo, H., and Poeppel, D. (2007). Phase patterns of neuronal responses reliably discriminate speech in human auditory cortex. Neuron *54*, 1001–1010.

MacNeilage, P.F., and Davis, B.L. (2000). On the origin of internal structure of word forms. Science *288*, 527–531.

MacNeilage, P.F., and Davis, B.L. (2001). Motor mechanisms in speech ontogeny: phylogenetic, neurobiological and linguistic implications. Curr. Opin. Neurobiol. *11*, 696–700.

Mandelkow, H., Halder, P., Boesiger, P., and Brandeis, D. (2006). Synchronization facilitates removal of MRI artefacts from concurrent EEG recordings and increases usable bandwidth. Neuroimage *32*, 1120–1126.

Mukamel, R., Gelbard, H., Arieli, A., Hasson, U., Fried, I., and Malach, R. (2005). Coupling between neuronal firing, field potentials, and FMRI in human auditory cortex. Science *309*, 951–954.

Obleser, J., Boecker, H., Drzezga, A., Haslinger, B., Hennenlotter, A., Roettinger, M., Eulitz, C., and Rauschecker, J.P. (2006). Vowel sound extraction in anterior superior temporal cortex. Hum. Brain Mapp. *27*, 562–571.

Peretz, I., and Zatorre, R.J. (2005). Brain organization for music processing. Annu. Rev. Psychol. *56*, 89–114.

Poeppel, D. (2003). The analysis of speech in different temporal integration windows: cerebral lateralization as 'asymmetric sampling in time'. Speech Commun. *41*, 245–255.

Rauschecker, J.P., and Tian, B. (2000). Mechanisms and streams for processing of "what" and "where" in auditory cortex. Proc. Natl. Acad. Sci. USA *97*, 11800–11806.

Rosen, S. (1992). Temporal information in speech: acoustic, auditory and linguistic aspects. Philos. Trans. R. Soc. Lond. B Biol. Sci. *336*, 367–373.

Ross, B., Herdman, A.T., and Pantev, C. (2005). Stimulus induced desynchronization of human auditory 40-Hz steady-state responses. J. Neurophysiol. *94*, 4082–4093.

Saberi, K., and Perrott, D.R. (1999). Cognitive restoration of reversed speech. Nature *398*, 760.

Schneider, P., Sluming, V., Roberts, N., Scherg, M., Goebel, R., Specht, H.J., Dosch, H.G., Bleeck, S., Stippich, C., and Rupp, A. (2005). Structural and functional asymmetry of lateral Heschl's gyrus reflects pitch perception preference. Nat. Neurosci. *8*, 1241–1247.

Scott, S.K., and Johnsrude, I.S. (2003). The neuroanatomical and functional organization of speech perception. Trends Neurosci. *26*, 100–107.

Traub, R.D., Buhl, E.H., Gloveli, T., and Whittington, M.A. (2003). Fast rhythmic bursting can be induced in layer 2/3 cortical neurons by enhancing persistent Na+ conductance or by blocking BK channels. J. Neurophysiol. *89*, 909–921.

Vertes, H.P. (2005). Hippocampal theta rhythm: a tag for short-term memory. Hippocampus *15*, 923–935.

White, L.J., and Plack, C.J. (1998). Temporal processing of the pitch of complex tones. J. Acoust. Soc. Am. *103*, 2051–2063.

Zatorre, R.J., and Belin, P. (2001). Spectral and temporal processing in human auditory cortex. Cereb. Cortex *11*, 946–953.